# Characteristics of the Chain Magnetic Film Storage Element

Abstract: This paper reports results of a detailed performance evaluation of the chain magnetic film storage element. The chains are made from copper strips which have been plated with a Ni-Fe film and are used to carry word current. The bit/sense signals are carried in wires which pass through the holes in the "links" of the chain. The memory element thus formed will operate in a rotational switching mode and can be used for a word-organized memory.

The results indicate both the advantages and the shortcomings of the device. Because of the complete flux closure, comparatively high output signal flux (200 mV-nsec) can be obtained from small, densely packaged devices which require less than 200 mÅ of word current and less than 100 mÅ of bit current. The chain shows high magnetic stability and can be operated in both a destructive and a nondestructive mode. The main problem is the difficulty in handling the delicate self-supporting magnetic devices, for testing, packaging, and wiring; this difficulty determines the limit of miniaturization.

Experimental results, including a large-scale reproducibility study, verify theoretical expectations,

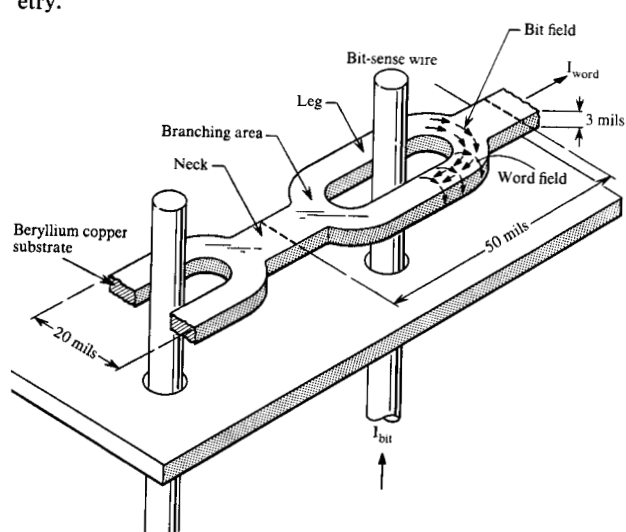
## Introduction

In the search for a memory device which combines the advantages of oriented magnetic film devices with the larger signals obtainable from ferrite cores, one looks for geometries which allow magnetic flux closure in both the word and the bit direction. The chain magnetic memory element<sup>1</sup> etched from solid permalloy sheets, as proposed by Sagnis, Stuckert, and Ward, is an approach toward this objective. Indeed, its surface fulfills nearly ideal conditions, but the inside portions are not exposed to uniform orthogonal drive fields. The device was therefore modified by etching the geometry (shown in Fig. 1) from beryllium copper sheets and plating the surface with a magnetic film.<sup>2</sup>

An external magnetic field, applied parallel to the longitudinal axis of the chain during the plating process, establishes a uniaxial anisotropy. The word current is carried by the chain itself. The bit field, orthogonal to the word line in the storage portion of the device (Fig. 1), is provided by a wire passing through the oblong hole in each element.

The operation of each surface element of the "leg" areas is similar to that for flat magnetic films; the word current rotates the magnetization into the hard-axis direction, causing a flux change which is detected by the bit/sense wire. A bit-current pulse provides an easy-axis

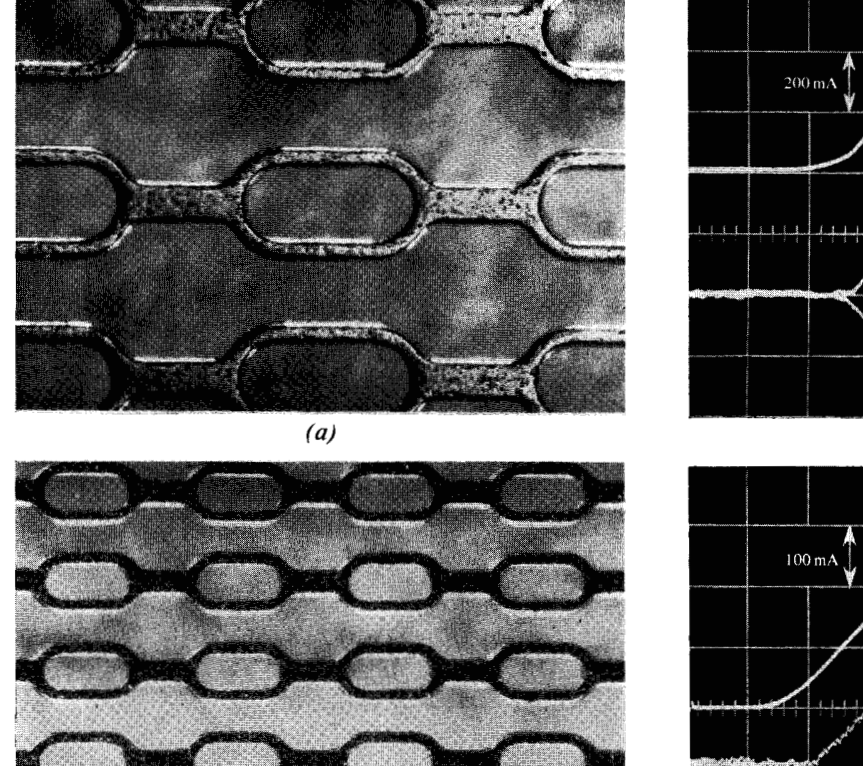
Figure 1 Chain store device configuration, Type E geometry.



field, so that after removal of the word current, the magnetization relaxes into the positive or negative easy direction, depending on the bit-pulse polarity.

The key to demonstrating the merits of the configuration was the development of a plating method for the deposition

291



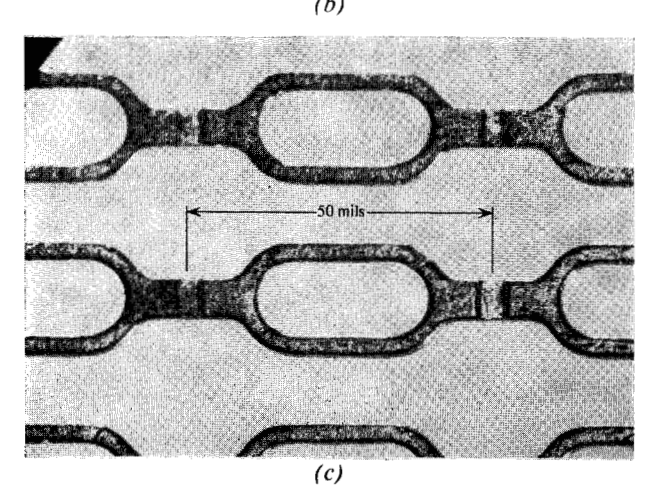
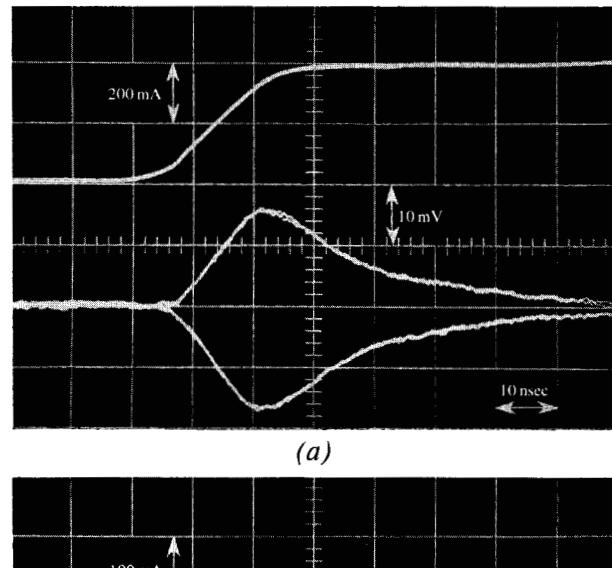


Figure 2 Chain devices: (a) Type E, (b) Mini-E, (c) Type E with interrupted neck.

of magnetic film on copper. A chemical deposition technique<sup>3</sup> yielded Ni-Fe films up to 30 kÅ thick, which satisfy the requirement of low dispersion (typically 2 degrees), a low anisotropy field ( $\approx$  4 oersteds), and sufficiently high coercive field (> 2 oersteds).



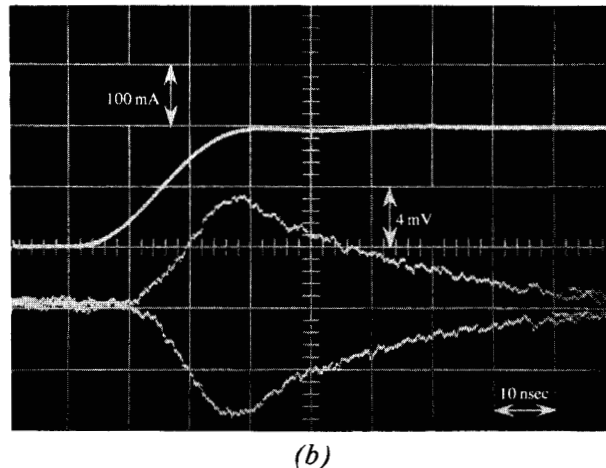


Figure 3 Word-read current and signal waveforms. (a) Type E (200 mA/cm, 10 mV/cm); (b) Mini-E (100 mA/cm, 4 mV/cm).

The basic advantages and disadvantages of the chain configuration will be discussed with respect to electrical operating conditions in a memory. The section titled *Chains as array elements* describes how the chain geometry determines the word and bit line characteristics. Device packaging requirements and problems are also discussed.

Experimental results are given, concerning destructive (DRO) and nondestructive (NDRO) modes and based on specific device dimensions (Type E, shown in Figs. 1 and 2a). Smaller devices (called Mini-E and shown in Fig. 2b) are also evaluated. The results of a successful reproducibility study conclude the paper.

# **Configurational characteristics**

# • Intrinsic advantages of flux closure

The major advantages of chains which result from their complete magnetic flux closure can be divided into two

categories: the absence of self-demagnetization and the absence of stray fields caused by the film magnetization. The lack of self-demagnetization of the stored flux implies that film thickness and device dimensions do not adversely affect the magnetization state and the disturb stability of the device. Therefore, very short path lengths can be used for low drive currents despite the use of rather thick films. The film thickness is limited only by the effects of eddy currents induced within film itself during fast rotational switching.4 A practical compromise between switching speed and signal flux was the selection of a film thickness of  $\delta = 20 \times 10^3 \text{ Å}$  with a damping time constant<sup>4</sup> of  $T_E =$  $(\delta^2 B_s)/(3\rho H_k) = 7$  nsec, and an output of  $\phi_{signal} = (B_s \cdot 1)$  $\delta \cdot \ell_w$ )/2 = 400 mVsec; this is based on the device dimensions of Type E chains and the following film parameters: flux density,  $B_s = 8 \times 10^3 G$ ; resistivity,  $\rho = 42 \mu \Omega$ -cm; anistotropy field,  $H_k = 4.6$  Oe; and word-field path length,  $\ell_w = 0.5$  cm. Figure 3a shows a signal waveform for "ones" and "zeros," together with the word-read current for a Type E chain. Figure 3b shows the corresponding waveforms for the miniaturized Mini-E device.

The advantages of using thick films as compared with the 500 to 1000 Å required for open-flux film devices are obvious, since 20 to 40 times more flux is available for the sense signals. This allows the use of relatively long rise times (20 nsec) and less expensive sense amplifiers. Lower signal frequency components also diminish transmission line losses so that longer lines can be permitted. For extremely fast memories, thinner films can be plated. For example, a 10,000 Å film yields 200 mV-nsec with a damping time constant of less than 2 nsec. The absence of self demagnetization of the word flux reduces the word current requirement to the theoretical minimum of  $I_w = H_w \cdot \ell_w$ .

The fact that the film magnetization does not contribute to stray fields drastically reduces the interaction among chains. Additionally, one can prove that the internal field of these small devices, with thick magnetic films, is considerably smaller than external stray fields. Accordingly, dynamic effects, such as flux trapping and image currents in surrounding metallic parts, are also minimized. One can therefore package chains very close to each other and to the ground conductors.

#### • Intrinsic problems of the chain structure

Inherently, in the mode of operation of the chain, the word current divides itself between the two legs. This doubles the word current required when compared with single-line devices having the same circumference as a single leg. In the "branching area" (Fig. 1), the bit and word fields are obviously no longer orthogonal to each other. A quantitative analysis of this effect is difficult since the surface is curved and the magnetic material is nonlinear. In addition, the film properties (easy-axis direction, anisotropy constant, dispersion, etc.) cannot be determined with sufficient

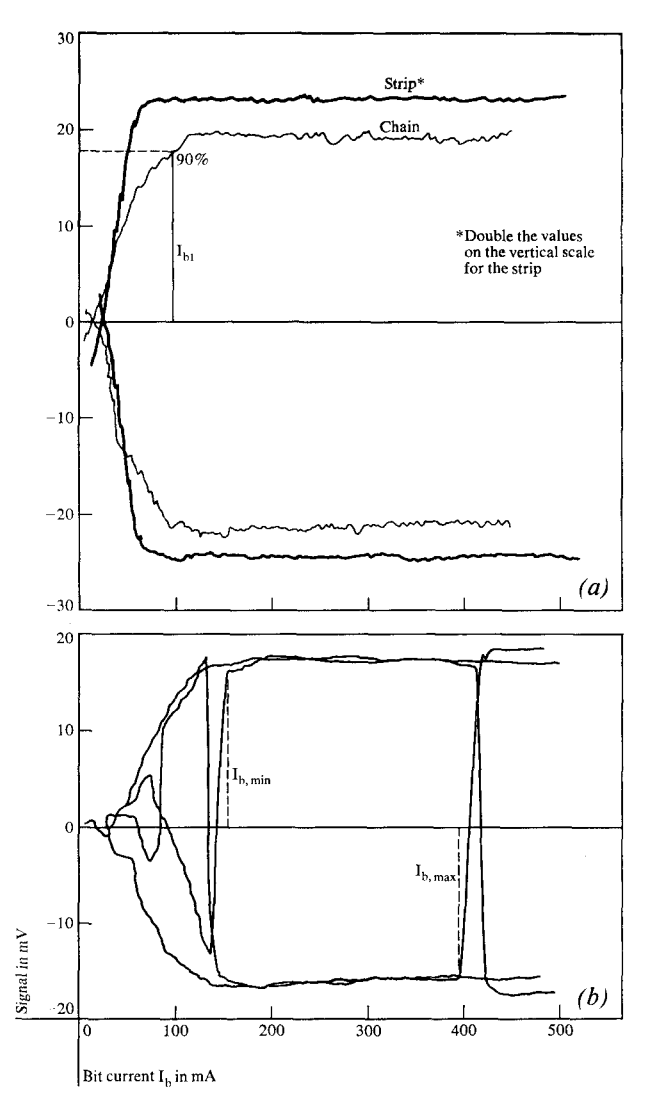


Figure 4 (a) The dispersion of strips and chains as measured on the undisturbed characteristic; (b) worst-case one-zero plot for Type E chain.

accuracy for quantitative predictions. An empirical approach was therefore chosen, and the entire branching area was regarded as a keeper between two short cylindrical rods, the "legs" in Fig. 1. The performance characteristics of the chain elements were compared with those of 1-inch long, 8-mil wide strips, etched and plated in the same manner, which provided the same performance characteristics as the film on the "legs."

The main result (Fig. 4a) of such a comparison is that the branching area apparently acts as a demagnetizing gap during the write operation, increasing the effective "device dispersion" by a factor of 2 to 3. Chains therefore share to a lesser extent some of the intrinsic disadvantages of film devices which do not have perfect, homogeneous closure of the easy-axis flux. Nevertheless, the degree of closure with the "plated keeper" by far exceeds that of

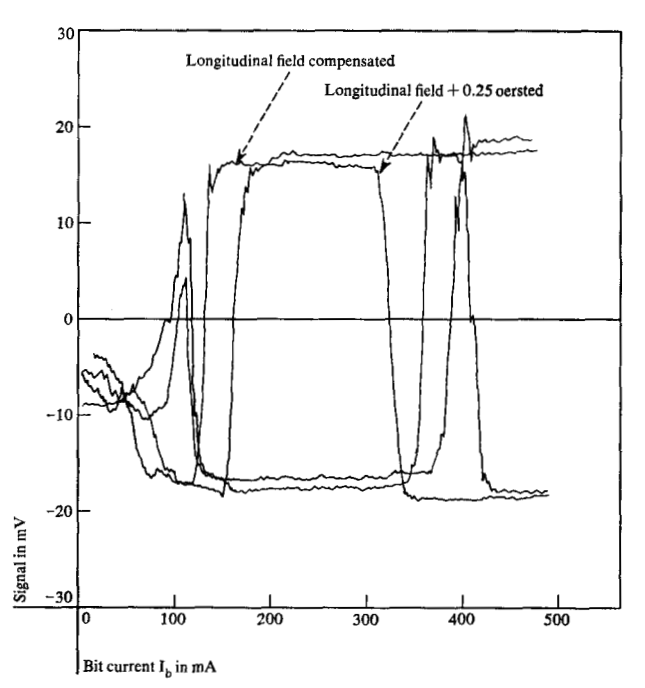


Figure 5 DRO one-zero plots for different values of longitudinal field.

corresponding air gaps and is independent of the film thickness.

The high disturb stability does not appear to be affected by the branching geometry shown. On the contrary, the strips consistently show lower bit-disturb thresholds due to domain-wall creepage from the ends of the sample towards its center.

Some dynamic effects resulting from noncoherent switching of the film in the branch area have been observed; for instance, the observed signal wave form deviates from the calculated. In addition, the dependence of disturb stability on the "overhang time," i.e., the duration of the bit pulse after the termination of the word pulse, is notable (Fig. 12). Neither phenomenon, however, significantly affects the usefulness of the chain as a high-speed memory element.

An external magnetic disturb field<sup>5</sup> parallel to the longitudinal axis of the chain, a so-called "longitudinal field," counteracts the bit field in one of the chain legs, and thereby increases the bit current required for complete device magnetization (Fig. 5). It also tends to diminish the disturb threshold. During nondestructive interrogation, however, the necks tend to align with the longitudinal field, and a kind of creep process begins in excessive fields. The tolerable field is therefore smaller in the NDRO mode (Fig. 6a), unless each neck is magnetically interrupted (Figs. 6b and 2c). Single-element measurements in a relatively long chain constitute the worst case in that the

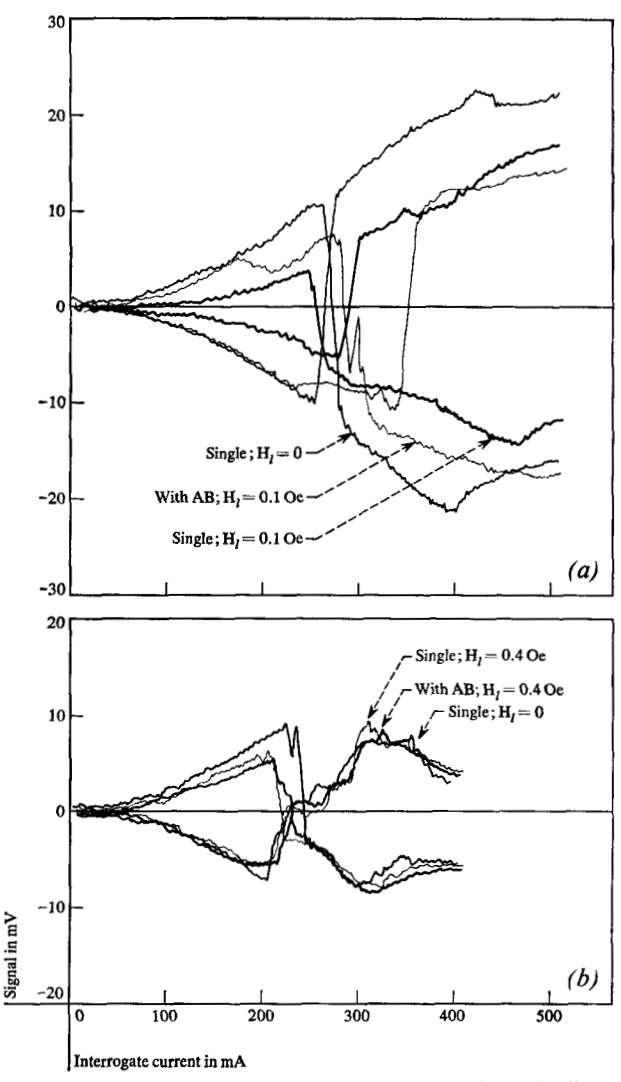


Figure 6 NDRO one-zero plots and the effect of longitudinal fields  $(H_t)$  for single-element measurements (Single), and for measurements with adjacent bits operated (with AB). (a) Continuously plated chain,  $H_t$  limit at 0.1 Oe, (b) interrupted neck chain,  $H_t$  limit at 0.4 Oe.

portions not subjected to bit fields, but only to word pulses, are extremely sensitive to longitudinal fields. Longitudinal flux sensing and field compensation are necessary under these test conditions.

Magnetic film interaction between adjacent elements on one chain has been measured (Fig. 7.) The nature of the results is similar to those from longitudinal field measurements. A 4-mil gap in the magnetic film on the neck considerably reduces adjacent element interaction.

## • Chains as array elements

If a chain is placed close to an insulated current-return plane, a strip transmission line with low stray inductance,  $(L_0$ , in the range of 0.06 nH per element), is obtained.

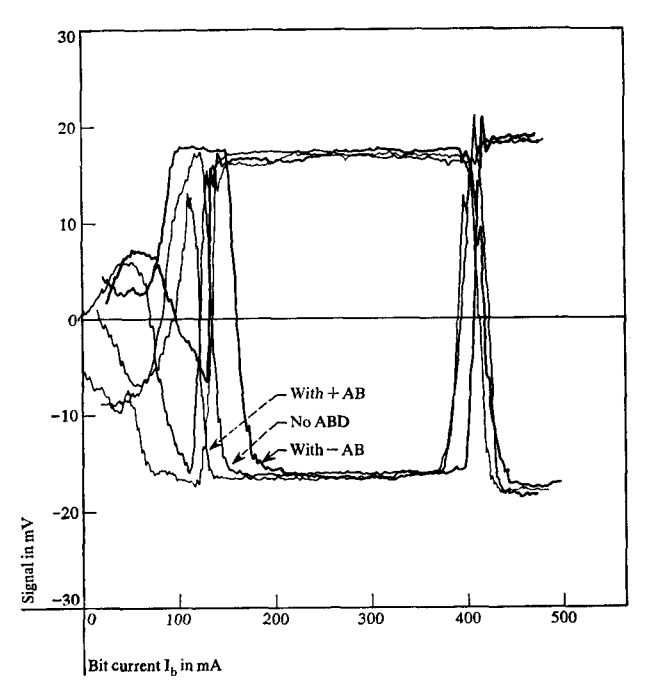


Figure 7 DRO one-zero plots with different polarities of adjacent bit currents (AB).

The word-line inductance for a single element is therefore dominated by the film inductance. For small word-field amplitudes  $(H_w < H_k)$ , the following equation can be expected where  $\ell_c$  is the length of each link (50 mils for Type E chains):

$$L_c = (B_s \delta \ell_c)/(H_k \ell_w).$$

If the previously mentioned values are used,  $L_c$  is 11nH. The eddy current theory<sup>4</sup> suggests that  $L_c$  is shunted by

$$R_c = L_c/T_E,$$

which would amount to  $1.56\Omega$ .

Experimentally, much smaller values<sup>5</sup> were found ( $L_c \approx 4$  nH,  $R_c \approx 0.5 \Omega$ ), which can be explained by imperfect switching in the neck and branching areas and by the nonlinearity and hard-axis locking of the magnetic material.

The expression  $L_c/(L_0 + L_c)$  characterizes the fraction of word field energy contained in the film as compared to the entire energy input. This energy efficiency ( $\approx 50\%$ ) is high when compared to open-flux storage devices, even though part of the film (branching and neck area) does not contribute to the storage mechanism.

The bit/sense line is a wire which penetrates the holes of the chain elements and holes in the word-current returns to form a dense laminated stack. The stray field inductance  $L_*$ , assuming a return wire in an adjacent stack, is in the range of 100 pH for #36 wires at a separation of 30 mils and a vertical spacing between chains of 10 mils. For

Mini-E chains, comparable values are 40 pH for #42 wires and 4-mil spacing. The fact that the space around the bitsense wires is partially filled with conductive material leads to even lower inductance values for high-frequency components, but it also causes frequency-dependent losses.

As a figure of merit, m, for the bit/sense line, one may consider the ratio of signal flux,  $\Phi_s$  to the stray flux,  $I_bL_s$ , generated by the bit current,  $i_B$ , per single (unswitched) element.

$$m = \Phi_{\bullet}/I_bL_{\bullet},$$

which amounts to 25 for Type E and Mini E chains. This high value of m reflects a favorable signal-to-write noise ratio for memory arrays.

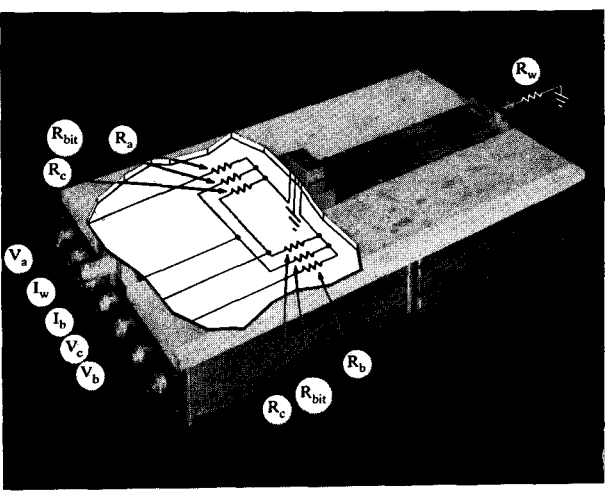
The magnetic film, aligned in its easy direction, has theoretically no effect on the bit-sense line inductance. In actual devices there is a contribution,  $L_F$ , due to easy-axis permeability;  $L_F$  also depends on the magnetization state of the device and thereby causes "information noise," which is similar to "delta-noise" in 3-D core arrays. Although the absolute value of  $L_F$  is small, it is significant since the stray field inductance  $L_s$  is also very small. The chain-to-wire capacitance per intersection, which plays an important role in the read noise, is as low as 0.006 to 0.015 pF.

These device properties are the basis for the array evaluation discussed in another paper.<sup>5</sup>

# Handling and packaging

The handling of small, thin, and oblong structures requires specific care. In the test fixtures, the chains were placed on an insulated ground plane and were contacted for word current with liquid metal (gallium, see Fig. 8).

Figure 8 Single-bit test fixture. Termination arrangement allows separate sensing of each leg  $(V_A \text{ and } V_B)$  for compensating longitudinal flux and common-mode voltage  $V_c = (V_A + V_B)/2$ .  $R_A = 50 \Omega$ ,  $R_{BIT} = 100 \Omega$ ,  $R_c = 100 \Omega$ ,  $R_w = 50 \Omega$ .



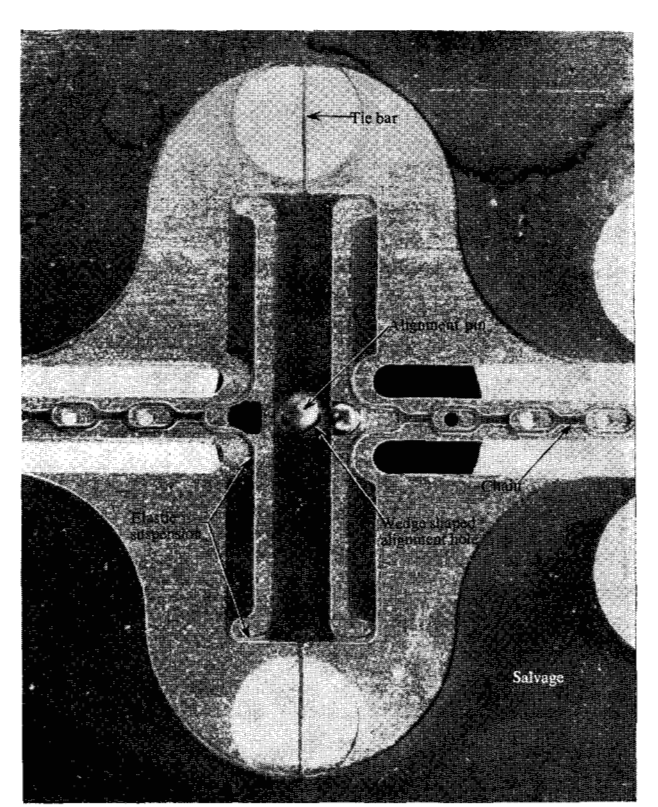
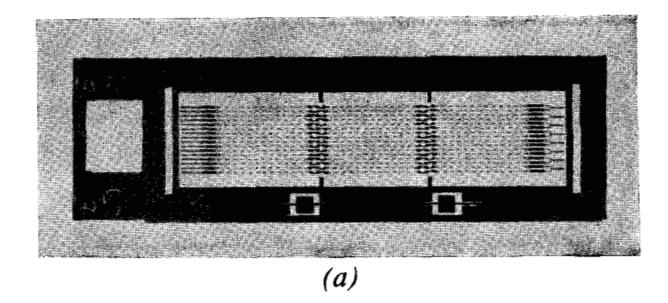


Figure 9 Suspension configuration for stress-free chain packaging and alignment over ground plane.



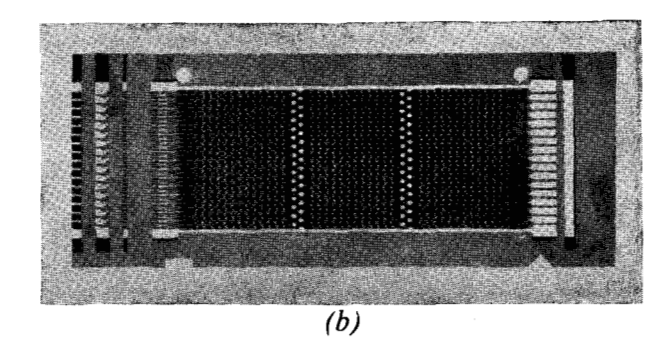
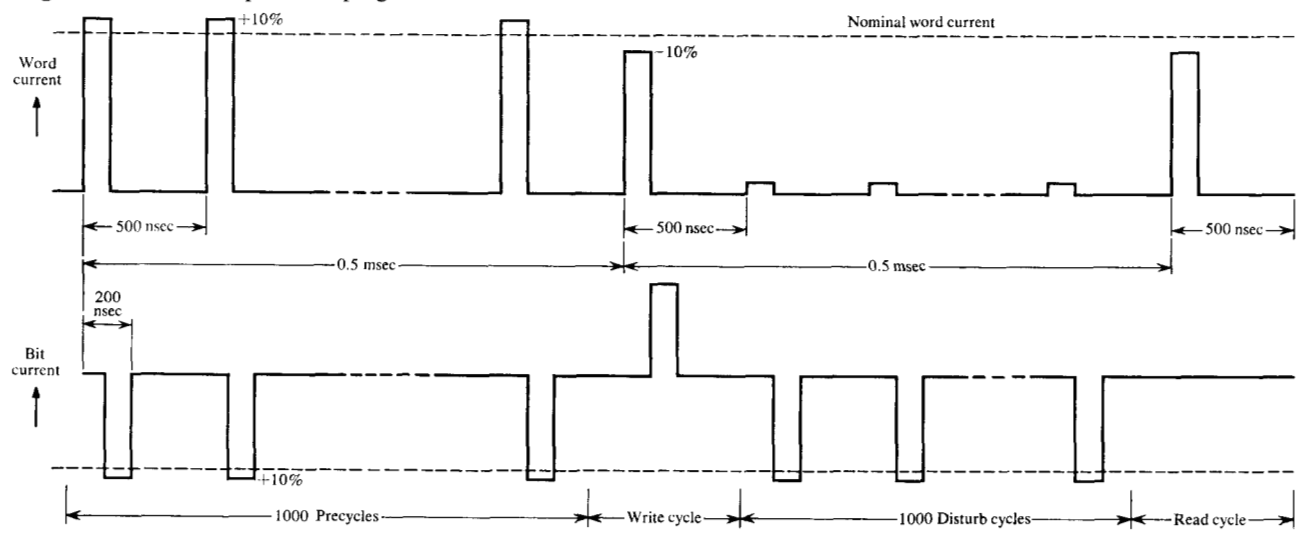


Figure 10 (a) Photograph of chain frame; (b) photograph of etched copper nest with chains welded in place.

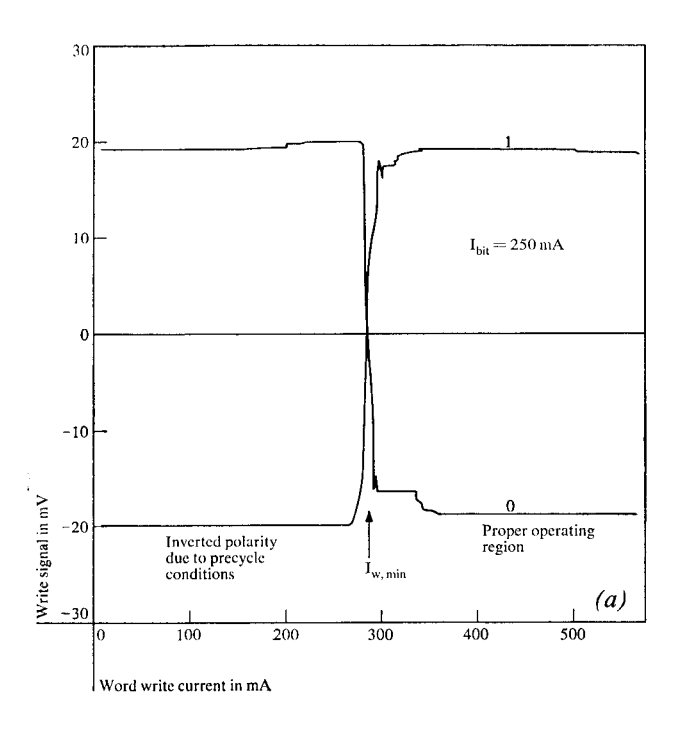
Figure 11 Worst-case pulse test program.



For the manufacture of chain memories, the chains must be manipulated with special tools, which must not touch or permanently stress the active device areas. By proper design of the photo-etching masks, one can provide auxiliary support elements such as tie bars, spring-like stress-relief elements, and alignment holes. The experimental configuration shown in Fig. 9 is an example of the

application of these possibilities. Word-drive connection density can be reduced by staggering the extended end tabs of adjacent laminates, thus allowing extremely small chain-to-chain distances.

An obvious way to batch-fabricate chains is to arrange the masks so that many chains can be etched and plated in parallel (see the yield study frame, Fig. 10).



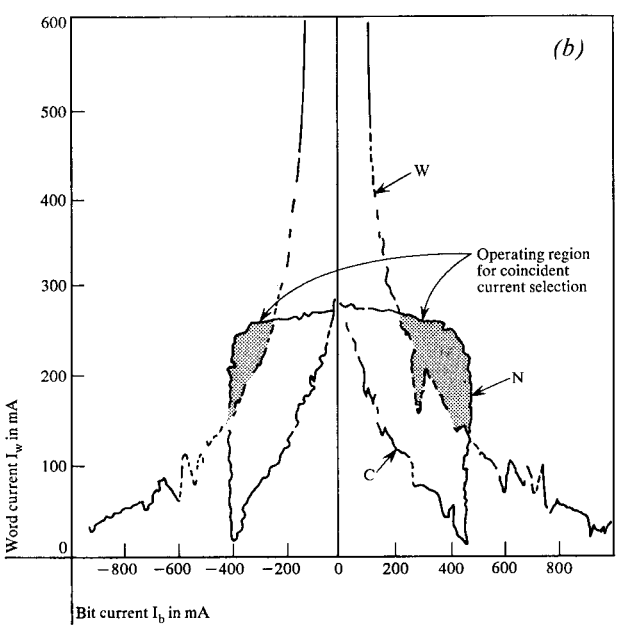


Figure 12 (a) Write characteristic for fixed bit current (250 mA); (b) asteroid illustrating the write characteristic W, coincident disturb characteristic C, and noncoincident disturb characteristic N.

# **Experimental results**

# • Destructive read-out evaluation

The basic test program (Fig. 11) simulates worst-case sequencing in memory operation. The write operation uses a unipolar word-current pulse of 400 mA, which is considered the low-margin value of a nominal amplitude. No detrimental locking effects were observed using very high

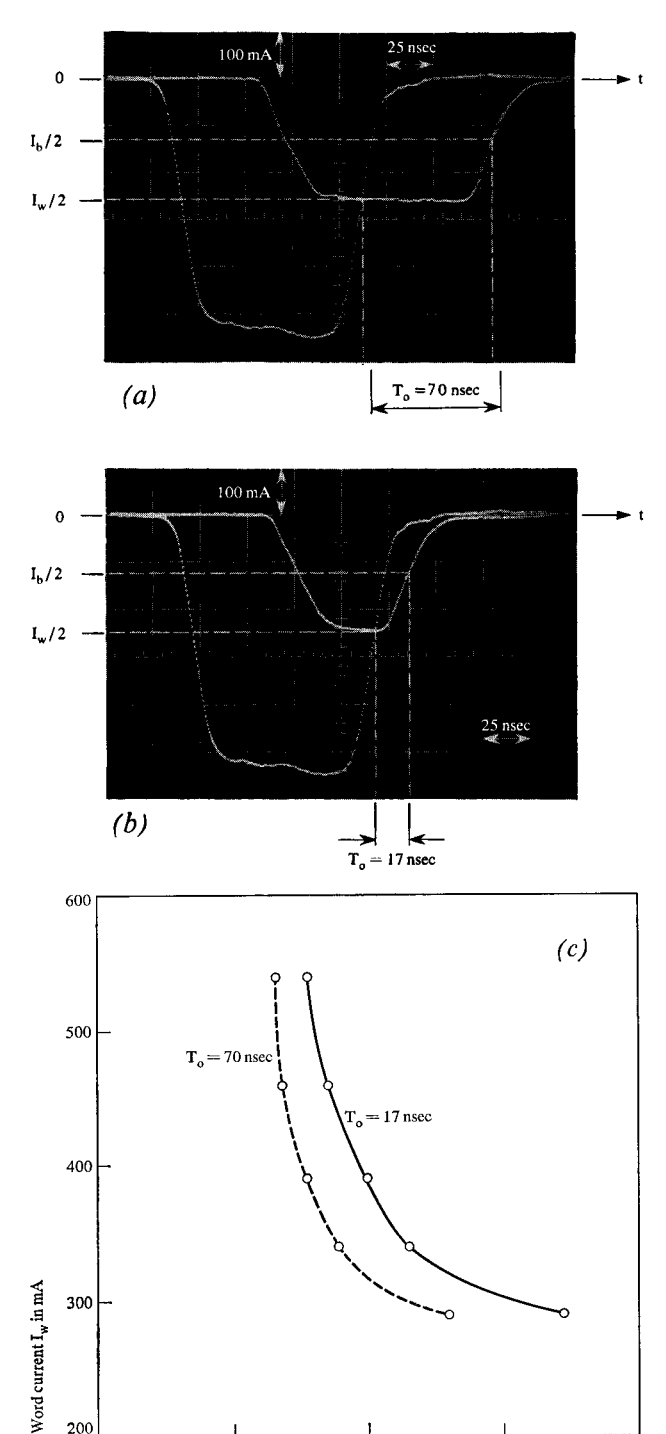
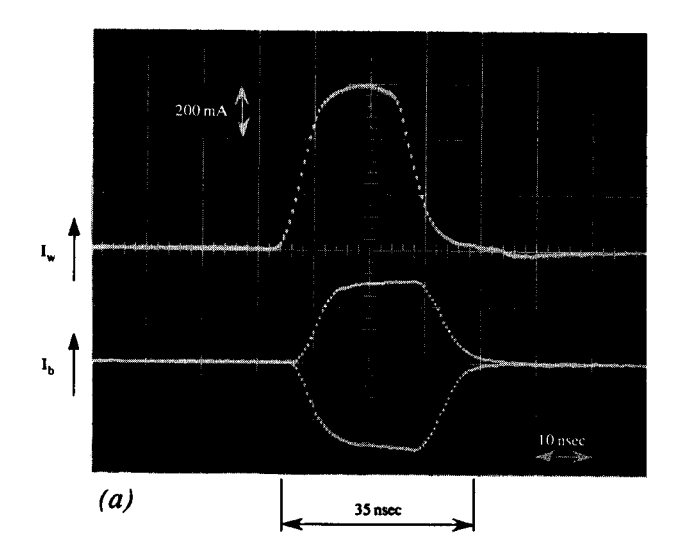


Figure 13 (a) Pulse conditions for a normal write cycle with a 70-nsec overhang; (b) pulse conditions for a faster write cycle with a 17-nsec overhang; (c) asteroid write characteristic to show the increase in word- and bit-current amplitudes required for the faster write cycle.

Bit current Ib in mA

word pulses (up to 1 ampere). The bit-write current was variable from 0 to 500 mA and was monitored to generate

400



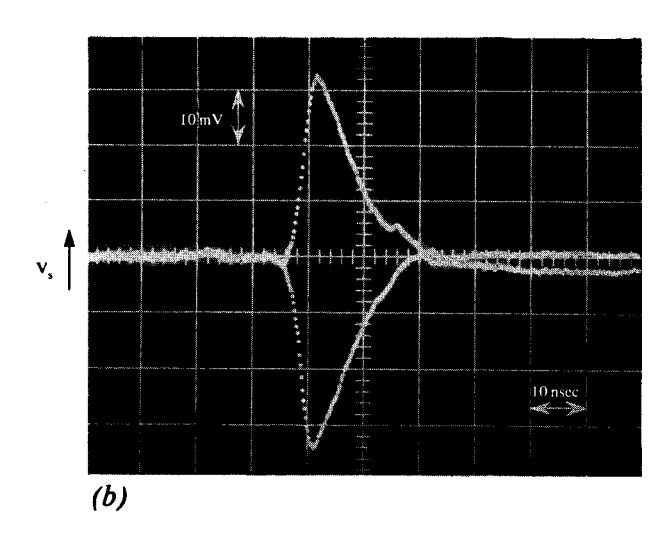
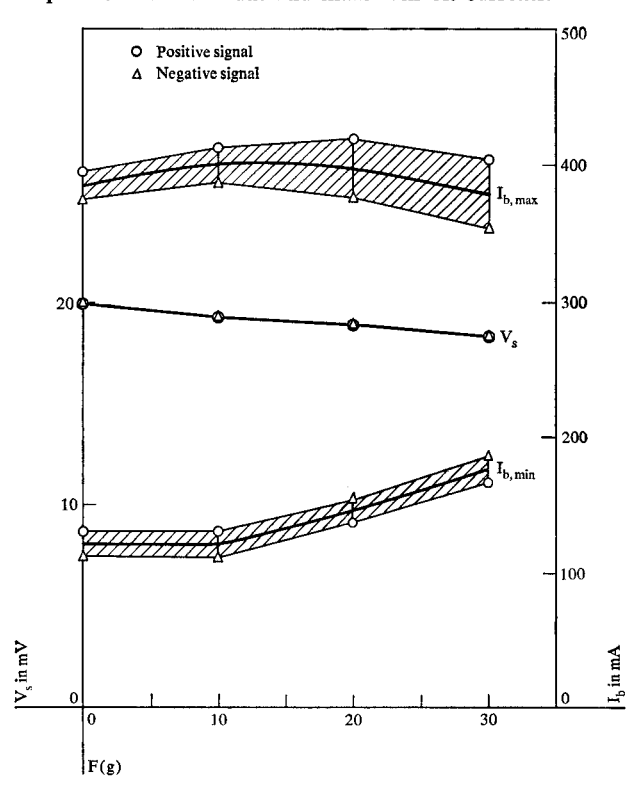


Figure 14 (a) Pulse conditions for a fast write cycle; (b) associated signal for a separate read pulse.

Figure 15 The effect of longitudinal stress on the signal amplitude and minimum and maximum bit currents.



the horizontal axis of the plot (Fig. 4b). The timing of word and bit pulses is shown in Fig. 13a.

Prior to the write operation, the device was conditioned by 1000 precycles. These are orthogonal-mode write operations with inverse bit currents which firmly magnetize the device in the opposite direction. These bit currents are 10% higher than the nominal value while the word-write current is 10% lower. Their ratio (1.22) is maintained over the entire plot.

The disturb phase consists of 1000 bit pulses at 110% of the nominal value in the opposite direction coincident with word-disturb currents of 30 mA amplitude, which corresponds to about 10% of  $H_k$  and represents possible leakage current in nonselected word lines.

The word-read current used is similar to the word-write current, and is shown in Fig. 3a, together with the signal waveform.

For bit current values up to  $I_{b1}$ , the undisturbed output signal increases and the magnetization state proves to be very disturb-sensitive, The dispersion<sup>6</sup> can be read from Fig. 4a to be

$$\alpha_{90 \text{ device}} = (I_{b1}\ell_w)/(I_k\ell_b) \approx 5.7^{\circ},$$

using the path lengths  $\ell_w=20$  mils and  $\ell_b=80$  mils. This is the effective device dispersion under application-type test conditions and includes device configuration effects. The "film dispersion" measured on strips under the same conditions is about  $2^\circ$  (see Fig. 4a and the discussion above).

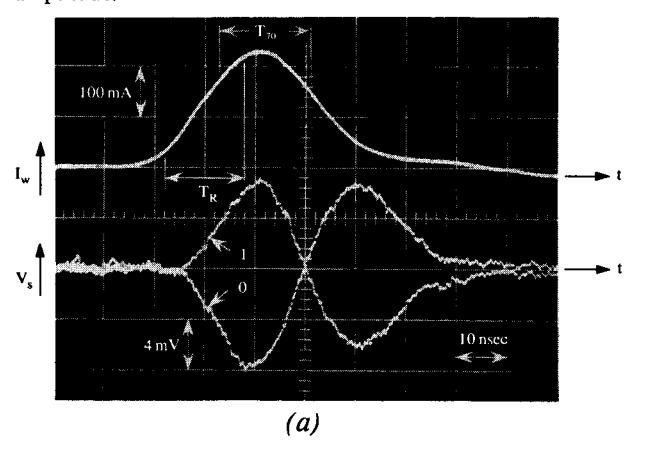
The device becomes magnetically stable when the bit current exceeds  $I_{b\ min}$  as shown by the constant amplitude of  $V_s$  in Fig. 4b.  $I_{b\ max}$  is the wall-motion threshold; 22% higher values are allowed since this margin is incorporated in the test.

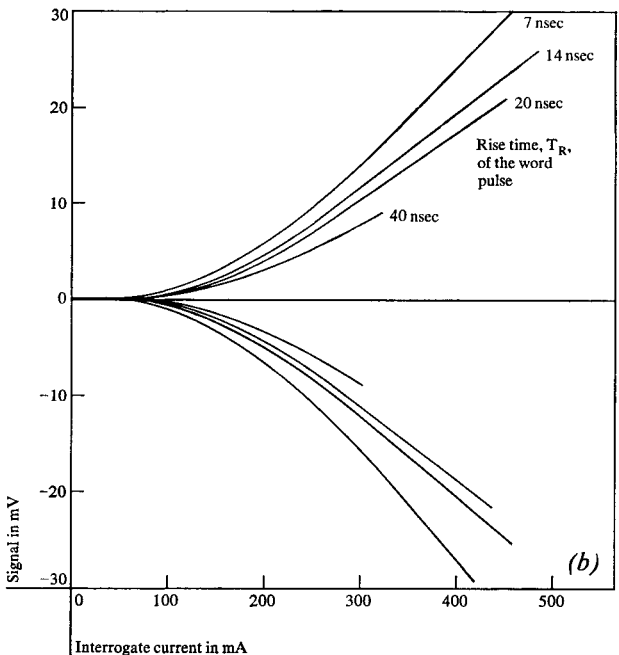
A plot of the amplitude of the word-write current shows (Fig. 12a) a similarly sharp threshold  $I_{wmin}$ , while lower currents have no effect upon the magnetization which has been previously fixed in the opposite direction.

Plotting  $I_{w\ min}$  versus  $I_{b\ min}$  (Fig. 12b, trace a) produces a very useful graph which corresponds to Stoner-Wohlfarth's "asteroid" presentation of switching threshold. This

asteroid relates actual device properties under worst-case application conditions. Also included in Fig. 12b are the thresholds for combinations of 1000 word- and bit-disturb pulses which in coincidence (trace b) and alternating non-coincidence (trace c) will destroy 10% of the written information. This gives the wall-motion threshold for the destructive read, nondestructive read, and coincident-current selection modes of operation (see next section). For these types of films, the wall motion threshold does not change as the number of disturb pulses increases (up to 10<sup>11</sup>). It has been verified that the signal waveforms are identical in all details if the peak voltages are equal.

Figure 16 (a) Current and signal voltage for the NDRO mode; (b) NDRO signal amplitude measured as a function of the read-pulse amplitude for different rise times; (c) NDRO signal measured as a function of the width of the interrogate-disturb pulse measured at 70% of its amplitude.





The pulse timing influences the minimum word and bit currents. If, for example, the "overhang time" (as defined in Figs. 13a and b) is changed, the asteroid is altered as shown in Figure 13c. The squareness of the one-zero plots is not affected. The magnetic cycle could be shortened to about 35 nsec (Fig. 14).

Since the films used were slightly magnetostrictive, it was decided to measure the overall effect of longitudinal forces F at the chains. Fig. 15 shows changes in  $I_{b\,max}$ ; and  $V_s$  for the measured sample, which are negligible up to about ten grams.

Temperatures between  $0^{\circ}$  and  $100^{\circ}$ C have little influence on the peak signal amplitudes, but higher temperatures lower  $H_k$  and thereby  $I_{b\,min}$  and  $I_{b\,max}$ . Aging at high temperatures ( $100^{\circ}$ C) under worst-case operational conditions has little effect on the device performance, since the films are annealed in an easy-axis field at high temperatures for a prolonged interval prior to testing.

#### Nondestructive read-out operation

A typical word-read pulse for NDRO and the corresponding signal waveform are shown in Fig. 16a. The signal amplitude  $V_{*max}$  depends upon the rise time and amplitude,  $I_{wmax}$ , of the word pulse. Experimental results are presented in Fig. 16b. The underlying theory is described and discussed by H. H. Zappe<sup>7</sup>, who also found a good correlation between the wall motion threshold  $i_0$  and the pulse width  $T_{70}$ , measured at 70% of the amplitude of the word-read current (see Fig. 16c).

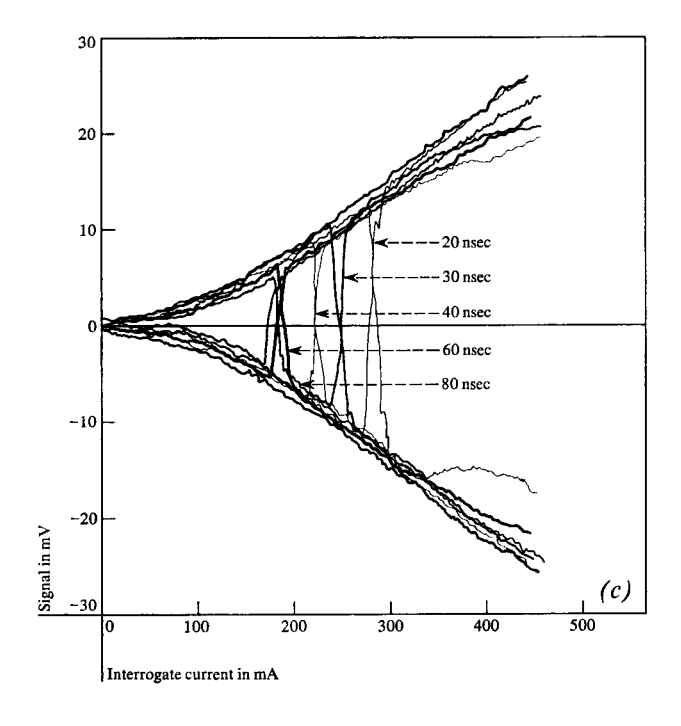


Table 1 Typical application specifications

Parameter	Dimension	Yield study specification	Type-E		Mini- $E$	
			high-speed	low-speed	high-speed	low-speed
Nominal word current (±10%)	mA	700	600	450	240	180
Word current rise time	nsec	20	5	20	5	20
Nominal bit current	mA	176	300	200	150	100
Bit current margins	%	$\pm 10$	$\pm 20$	$\pm 20$	$\pm 20$	$\pm 20$
Minimum DRO signal	mV	$\pm 10$	$\pm 20$	$\pm 10$	±8	±4
Magnetic cycle time	nsec	200	40	200	40	200
NDRO read current (±10%)	mA	_	220	220	90	90
NDRO current rise time	nsec		7	15	7	15
NDRO current width (70%)	nsec		20	20	20	20
Minimum NDRO signal	mV		±8	±5	$\pm 3$	±2
Maximum longitudinal field				_		
(DRO, without neck interruption)	Oe	_	0.25	0.25	0.25	0.25
Longitudinal force	gm	_	10	10	3	3
Temperature range	°C	25	0-100	0-100	0-100	0-100

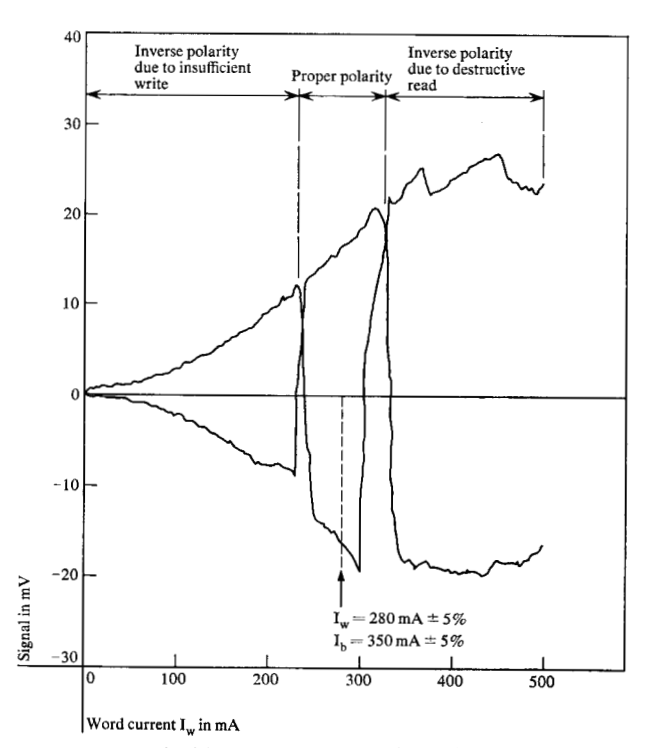


Figure 17 Coincident-current operation plot (same word pulses used for read, write, and disturb).

The NDRO test program includes 1000 word-disturb pulses, which are 22% higher than the read pulses, interleaved with the 1000 disturb cycles in the DRO test program (Fig. 11). This proved to be a more rigorous test than consecutive bursts of word and bit currents.

If the nondestructive read current in coincidence with the bit current is able to set the device in a stable state, while word and bit currents alone will not disturb the magnetic state, the element will be capable of coincident

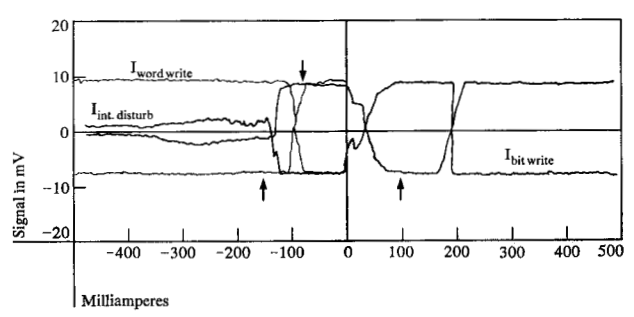


Figure 18 One-zero plot of a Mini-E chain showing the signal amplitude as a function of the word, the bit, and the interrogate current. Two variables are fixed at indicated values, while the remaining one is varied.

current selection. This feature, while allowing a very attractive memory organization<sup>8</sup>, requires very high quality devices. It has been demonstrated, on several devices, that chains can perform in this way in an operational test program, yet the margins allowable for word and bit currents are rather small ( $\pm$  5%). Figure 17 shows an NDRO plot where the same word-current pulse was used for precycle, write cycle, and read cycle. The disturb cycle included 1000 alternate word and bit currents. The bit currents required were very high (350 mA  $\pm$  5%). The operational range for word and bit currents can be seen quite clearly from the asteroid plot (Fig. 12b).

# Miniature chains

The Mini-E (half-size Type E) chains were produced (Fig. 2b) by photographic reduction of the chain mask. Their properties were found to be very similar with respect to disturb stability, NDRO properties, and even coincident current capabilities at reduced current and signal levels. Fig. 18 shows a composite plot of signal versus bit currents (± 20% margins included), word-write current, and

NDRO disturb currents. The arrows indicate the values of two of the variables and the signal is plotted against the remaining variable.

Based on the measurements performed, there appears to be no micromagnetic mechanism that precludes the assumption that all characteristics obtained from larger samples can be applied to miniaturized devices with the appropriate scaling factor. Table 1 is a list of consistent specifications which are met by the chain element. The data from previously plated samples used for the reproducibility study, as well as the data from large samples, are included.

# Reproducibility

When the feasibility of the basic idea was demonstrated and the process for producing chains subsequently refined, an extensive yield study was initiated on a pilot-line basis. The package (Fig. 10) for this study was a copper-epoxyglass-copper laminate with one side etched to provide a nest for the chains, and the other side etched to provide the return path for the word current. Thirty-two chains of thirty-six bits each were welded to the plane for a total of 1152 bits. Each bit of this assembled package was tested in an automatic handler, and the individual signal amplitudes were recorded on punched cards. Extensive computer assitance was employed in analyzing the data from the plane study to pinpoint failure mechanisms and improve yield. The pulse specifications for the automatic plane tester were similar to those described (see Fig. 11). Only the destructive read-out properties of the chain were tested and evaluated.

A plane was accepted only when all 1152 devices had signal magnitudes of more than 10 mV. Of 36 planes tested in the main run, 25 (70%) were acceptable in the first test. Another 8 planes were repaired by replacing a few word lines to raise the yield to 91.5%.

# **Conclusions**

This evaluation of the chain element reveals the advantage of full flux closure in word and bit dimensions for a storage application. In addition, the chain element demonstrates high stability with respect to disturb pulses, mechanical stress, temperature, and time; high yield in the plane package, and feasible miniaturization without penalty to electromagnetic performance. Difficulties inherent in the branching geometry and the longitudinal field sensitivity have been brought under control.

Key problems remain, however, in the fabrication, evaluation, and utilization of chains. These result from the necessity to plate the entire surface of the device, and consequently, to handle delicate parts, to assemble them into a solid package, and to wire and connect them.

# **Acknowledgements**

The authors wish to acknowledge the contributions of Dr. N. W. Silcox, Mr. H. Koretzky, Dr. L. Romankiw, Mr. O. Gutwin, Mr. G. J. Kahan, Mr. W. H. Rhodes, Jr., and Dr. W. B. Ittner III. Thanks are also due Mr. M. E. Deckert who performed most of the measurements in this paper. Other contributions are mentioned in the references.

#### References

- J. C. Sagnis, P. E. Stuckert, and R. L. Ward, "The Chain Magnetic Memory Element," IBM Journal 9, 412 (1965).
- H. O. Leilich, "The Chain—A New Magnetic Film Memory Device," Journ. Appl. Phys. 37, 1361 (1966).
   A. F. Schmeckenbecher, "Chemical Nickel-Iron Films,"
- A. F. Schmeckenbecher, "Chemical Nickel-Iron Films,"
   Extended Abstracts of Electrodeposition Division (The Electrochemical Society, Inc., N. Y. 1965), Vol. 8, pp. 19-23.
  H. O. Leilich, H. S. Hou, and H. H. Zappe, "Eddy Currents
- H. O. Leilich, H. S. Hou, and H. H. Zappe, "Eddy Currents in Rotational Switching of Oriented Magnetic Films," *Proc. Intermag. Conference*, Washington, D. C. (1965), 5. 7-1.
- S. A. Abbas, H. F. Koehler, T. C. Kwei, H. O. Leilich and R. H. Robinson, "Design Considerations for the Chain Magnetic Storage Array," IBM Journal 11, 302 (this issue).
- H. S. Belson, "Measurement of Skew, Dispersion and Creep in Plated Wires," Proc. Intermag. Conference, Washington, D. C. (1963), 12, 4.1.
- H. H. Zappe, "Nondestructive Readout in Thick Magnetic Film Devices," *IEEE Trans. Magnetics* Mag-3, 2 (1967).
- 8. W. J. Bartik, C. D. Chong, and A. Turczyn, "A 100-Megabit Random Access Plated-Wire Memory," *Proc. Intermag. Conference*, Washington, D. C. (1965), 11, 5-1.

Received August 4, 1966.